Available online at www.sciencedirect.com
SCIENCE DIRECT®
Advances in Space Research 36 (2005) 694–697
ADVANCES IN SPACE RESEARCH (a COSPAR publication)
www.elsevier.com/locate/asr

# Clusters of galaxies: new results from the CLEF hydrodynamics simulation

S.T. Kay [a,*], A.C. da Silva [b], N. Aghanim [b], A. Blanchard [c], A.R. Liddle [a], J.-L. Puget [b], R. Sadat [c], P.A. Thomas [a]

[a] Astronomy Centre, University of Sussex, Falmer, Brighton BN1 9QH, UK
[b] IAS, Bâtiment 121, Université Paris Sud, F-91405 Orsay, France
[c] Observatoire Midi-Pyrénées, Av. Edouard Belin 14, F-31500 Toulouse, France

Received 24 September 2004; received in revised form 22 November 2004; accepted 26 November 2004

**Abstract**

Preliminary results are presented from the CLEF hydrodynamics simulation, a large ($N = 2 \times 428^3$ particles within a 200 $h^{-1}$ Mpc comoving box) simulation of the ΛCDM cosmology that includes both radiative cooling and a simple model for galactic feedback. Specifically, we focus on the X-ray properties of the simulated clusters at $z = 0$ and demonstrate a reasonable level of agreement between simulated and observed cluster scaling relations.


*Keywords:* Cosmology; Clusters of galaxies; X-ray, Numerical simulations; Hydrodynamics; Galaxy formation

## 1. Introduction

As the largest and latest virialised structures to form, galaxy clusters are especially useful cosmological probes (e.g. see Viana et al., 2003, and references therein). Next generation cluster cosmology surveys, such as the XCS (Romer et al., 2001), will detect sufficiently large numbers of clusters that uncertainties in values of cosmological parameters will be mainly systematic, requiring for example an accurate calibration between cluster X-ray temperature and mass. Such measurements demand an improved understanding of cluster physics, therefore realistic numerical simulations of the cluster population are essential.

In this paper, we present a preliminary analysis of the $z = 0$ cluster population within the CLEF hydrodynamics simulation, a large state-of-the-art cosmological simulation that, besides gravity and gas dynamics, includes a model for the effects of galaxy formation. As we will show, the simulation does a reasonably good job at reproducing X-ray scaling relations at $z = 0$.

## 2. The CLEF hydrodynamics simulation

The CLEF (CLuster Evolution and Formation) hydrodynamics simulation (see Fig. 1) is a large simulation of structure formation within the ΛCDM cosmology, with the following cosmological parameters: $\Omega_m = 0.3$, $\Omega_\Lambda = 0.7$, $\Omega_b h^2 = 0.0238$, $h = 0.7$ and $\sigma_8 = 0.9$. These values are in good agreement with recent *WMAP* analyses (Spergel et al., 2003).

Initial conditions were generated using a modified version of the COSMICS software package provided with the HYDRA code (Couchman et al., 1995). The appropriate

* Corresponding author. Present address: Astrophysics, Denys Wilkinson Building, Keble Road, OX1 3RH Oxford, UK. Tel.: +44 1865 273 298; fax: +44 1865 273 390.
*E-mail addresses:* s.t.kay@sussex.ac.uk (S.T. Kay), skay@astro.ox.ac.uk (S.T. Kay).

0273-1177/$30 
doi:10.1016/j.asr.2004.11.034

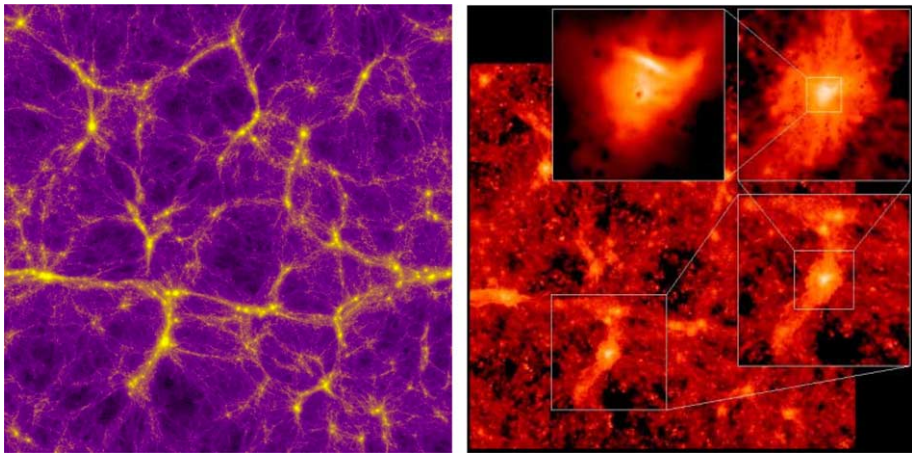

Fig. 1. Left: optical depth image of the gas in a $200 \times 200 \times 10\ h^{-1}$ Mpc slice at $z = 0$. Right: series of zooms showing images of the mass-weighted temperature of the gas, from the full box width to an individual cluster.

transfer function, generated using CMBFAST (Seljak and Zaldarriaga, 1996), was read in and a displacement field generated for a $200\ h^{-1}$ Mpc comoving box at $z = 49$. Two regular cubic grids of $428^3$ particles, separated by half the interparticle distance in each of the $x$, $y$ and $z$ directions, were then perturbed by these displacements to create the initial particle positions. Thus, the gas and dark matter particle masses were set to $m_{\rm gas} = 1.4 \times 10^9\ h^{-1}\ M_\odot$ and $m_{\rm dark} = 7.1 \times 10^9\ h^{-1}\ M_\odot$, respectively.

This initial configuration was then evolved to $z = 0$ using version 2 of the GADGET code (Springel et al., 2001), a hybrid Particle-Mesh/Tree gravity solver with a version of Smoothed Particle Hydrodynamics (SPH) that explicitly conserves entropy where appropriate. In addition, the gas could cool radiatively, assuming a fixed metallicity of $Z = 0.3\ Z_\odot$. Cooled gas, with $n_{\rm H} > 10^{-3}\ {\rm cm}^{-3}$ and $T < 1.2 \times 10^4$ K, could either form stars if $r > f_{\rm heat}$ or be reheated by stars if $r < f_{\rm heat}$, where $r$ is a random number drawn for each particle from the unit interval and $f_{\rm heat} = 0.1$ is the reheated mass fraction parameter. Each reheated gas particle was given a fixed amount of entropy, $S_{\rm heat} = 1000$ keV cm$^2$, where $S \equiv kT/n^{2/3}$, which further heats the ICM as the particle does work on its surroundings. Further details may be found in Kay et al. (2004).

## 3. X-ray scaling relations at $z = 0$

In this paper, we concentrate on comparing a selection of simulated and observed X-ray cluster scaling relations at $z = 0$. Clusters were identified by first identifying local maxima in the density field and growing spheres around these maxima until the average density within each sphere was a fixed factor, $\Delta$, above the critical density, $\rho_{\rm cr} = 3H_0^2/8\pi G$. Values of $\Delta$ used will be given in each subsection. For the virial density ($\Delta \sim 104$) there are >400 clusters with $kT_{\rm vir} > 1$ keV (>60 above 3 keV).

### 3.1. Temperature–mass relation

We begin by showing in Fig. 2 the relation between hot gas mass-weighted temperature ($T_{\rm gas} \equiv \sum_i m_i T_i / \sum_i m_i$, where the sum is over all gas particles with $T_i > 10^5$ K) and total mass for a density contrast $\Delta = 2500$. All clusters with $M_{2500} > 3 \times 10^{14}\ h^{-1}\ M_\odot$ are considered. The dashed line is a best-fit relation to the clusters for a fixed slope of 2/3, as expected if the clusters form a self-similar population. This relation is

$$\log(kT_{\rm gas}/{\rm keV}) = (0.614 \pm 0.003) + (2/3) \times \log(M_{2500}/M_{14}), \quad (1)$$

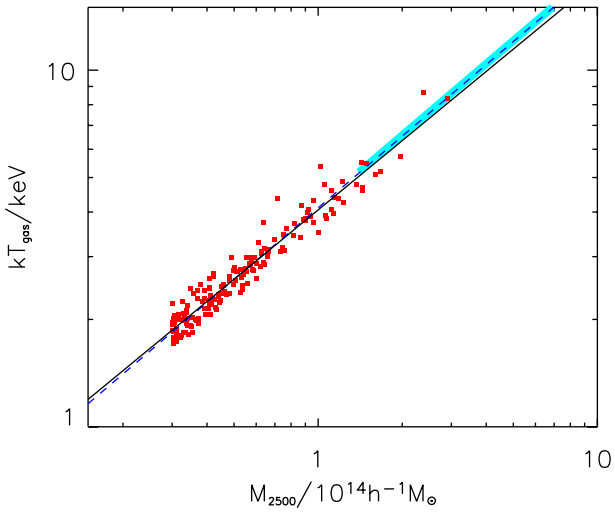


Fig. 2. Gas mass-weighted temperature versus mass, evaluated at $\Delta = 2500$. The dashed line is the best-fit relation with the self-similar slope 2/3. The solid line is the best-fit relation, allowing both the normalisation and slope to vary. The solid band is the best-fit relation to clusters studied by Allen et al. (2001).

where $M_{14} = 10^{14}\,h^{-1}\,M_{\odot}$. When the slope is allowed to vary, the best-fit relation (solid line) is

$$\log(kT_{\rm gas}/{\rm keV}) = (0.608 \pm 0.004) + (0.65 \pm 0.01) \times \log(M_{2500}/M_{14}), \quad (2)$$

close to the self-similar relation. The thick band is the observed relation derived by Allen et al. (2001), in good agreement with our results.

It is more common in the literature for observed temperature–mass relations to be presented at larger radii, using spectroscopic (photon-weighted) temperatures and mass estimates assuming β-model surface brightness profiles and polytropic-model temperature profiles (e.g., Nevalainen et al., 2000; Finoguenov et al., 2001; Sanderson et al., 2003). These results generally suggest a slope closer to 1/2 than 2/3, attributed to non-gravitational processes (see below), and a normalisation that is offset in mass from simulation predictions by ~40%. Examining, for example, the X-ray emission-weighted temperature–mass relation from our simulation at $r_{500}$, $T_{\rm X} - M_{500}$ [$T_{\rm X} \equiv \sum_i m_i n_i\ \Lambda(T_i) T_i / \sum_i m_i n_i \Lambda(T_i)$, where $\Lambda$ is an energy-dependent cooling function], we find a similar slope to the observations (0.53) but an offset in normalisation comparable to previous simulations. The cause of this offset is likely due to incorrect estimates of cluster masses (e.g., Rasia et al., 2005) and is something we will return to in a future paper.

### 3.2. Entropy–temperature relation

Galaxy formation increases the entropy of intracluster gas, producing a relationship with temperature that is flatter than the self-similar scaling ($S \propto T$). We plot this relation in Fig. 3, again using an X-ray emission-weighted temperature for each cluster. Two radii are considered ($0.1r_{200}$ and $r_{500}$) and only clusters with $kT_{\rm X} > 1$ keV are studied. Again, the simulated clusters are in reasonably good agreement with the observations (Ponman et al., 2003), containing an excess of entropy that is larger in smaller systems. For $0.1r_{200}$

$$\log(S/{\rm keV\ cm^2}) = (2.14 \pm 0.008) + (0.46 \pm 0.03) \times \log(kT_{\rm X}/{\rm keV}) \quad (3)$$

and for $r_{500}$

$$\log(S/{\rm keV\ cm^2}) = (2.84 \pm 0.003) + (0.63 \pm 0.01) \times \log(kT_{\rm X}/{\rm keV}). \quad (4)$$

### 3.3. Luminosity–temperature relation

Finally, we show bolometric X-ray luminosity versus X-ray emission-weighted temperature in Fig. 4. Again, only clusters with $kT_{\rm X} > 1$ keV are considered. Symbols with errors are observational data from Markevitch (1998) and Arnaud and Evrard (1999). To remain approximately consistent with this data, emission from within $50\,h^{-1}$ kpc of our simulated cluster centres is omitted.

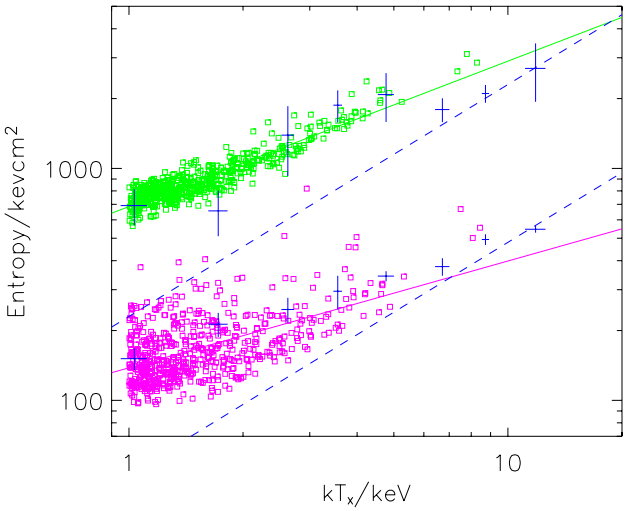


Fig. 3. Entropy versus X-ray emission-weighted temperature at $0.1r_{200}$ (lower points) and $r_{500}$ (upper points), with the solid lines being fits to these data. Crosses are data from Ponman et al. (2003) and dashed lines are self-similar scalings, normalised to their hottest clusters.

The dashed line is a best-fit relation for a fixed slope equal to 2 (self-similar), clearly a poor fit to the observations. When the slope is allowed to vary, the best-fit relation (solid line) is

$$\log(L_{\rm X}/L_{40}) = (1.89 \pm 0.01) + (3.84 \pm 0.05) \times \log(kT_{\rm X}/{\rm keV}), \quad (5)$$

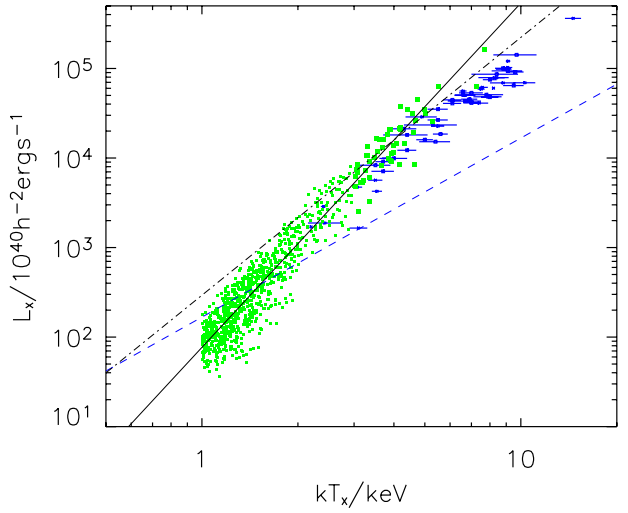


Fig. 4. Bolometric X-ray luminosity versus emission-weighted temperature in 1.5–8.0 keV band. Symbols with error bars are data from Markevitch (1998) and Arnaud and Evrard (1999). The dashed line is the best-fit relation for a fixed slope of 2. The solid line is the best-fit relation for $kT_{\rm X} > 1$ keV and the dot-dashed line for $kT_{\rm X} > 3$ keV.

where $L_{40} = 10^{40}\,h^{-2}\,erg\,s^{-1}$, considerably steeper than the self-similar case. In fact, the simulated relation is not adequately described by a power law since the local gradient becomes progressively flatter with increasing temperature. Fitting clusters with $kT_X > 3$ keV (dot-dashed line) yields

$$\log(L_X/L_{40}) = (2.47 \pm 0.03) + (2.88 \pm 0.05) \times \log(kT_X/\mathrm{keV}), \quad (6)$$

in reasonable agreement with the observations although the normalisation is a bit too high. Better agreement was reached by Kay et al. (2004), who used a slightly smaller gas fraction (0.15 rather than 0.162 used here, which is a closer match to the *WMAP* value). It is likely however that fine tuning of the feedback model parameters would improve the agreement between the simulated and observed relations.

## References


Allen, S.W., Schmidt, R., Fabian, A.C. The X-ray virial relations for relaxed lensing clusters observed with Chandra. MNRAS 328, L37–L41, 2001.

Arnaud, M., Evrard, A.E. The $L_X$–$T$ relation and intracluster gas fractions of X-ray clusters. MNRAS 305, 631–640, 1999.

Couchman, H.M.P., Thomas, P.A., Pearce, F.R. Hydra: an adaptive-mesh implementation of $P^3$M-SPH. ApJ 452, 797–813, 1995.

Finoguenov, A., Reiprich, T.H., Böhringer, H. Details of the mass–temperature relation for clusters of galaxies. A&A 368, 749–759, 2001.

Kay, S.T., Thomas, P.A., Jenkins, A., Pearce, F.R. Cosmological simulations of the intracluster medium. MNRAS 355, 1091–1104, 2004.

Markevitch, M. The $L_X$–$T$ relation and temperature function for nearby clusters revisited. ApJ 504, 27–34, 1998.

Nevalainen, J., Markevitch, M., Forman, W. The cluster $M$–$T$ relation from temperature profiles observed with ASCA and ROSAT. ApJ 532, 694–699, 2000.

Ponman, T.J., Sanderson, A.J.R., Finoguenov, A. The Birmingham-CfA cluster scaling project 0- III. Entropy and similarity in galaxy systems. MNRAS 343, 331–342, 2003.

Rasia, E., Mazzotta, P., Borgani, S., Moscardini, L., Dolag, K., Tormen, G., Diaferio, A., Murante, G. Mismatch between X-ray and emission-weighted temperatures in galaxy clusters: cosmological implications. ApJ 618, L1–L4, 2005.

Romer, A.K., Viana, P.T.P., Liddle, A.R., Mann, R.G. A serendipitous galaxy cluster survey with XMM: expected catalog properties and scientific applications. ApJ 547, 594–608, 2001.

Sanderson, A.J.R., Ponman, T.J., Finoguenov, A., Lloyd-Davies, E.J., Markevitch, M. The Birmingham-CfA cluster scaling project-I. Gas fraction and the $M$–$T_X$ relation. MNRAS 340, 989–1010, 2003.

Seljak, U., Zaldarriaga, M. A line-of-sight integration approach to cosmic microwave background anisotropies. ApJ 469, 437–444, 1996.

Spergel, D.N., et al. (the WMAP team). First-year Wilkinson microwave anisotropy probe (WMAP) observations: determination of cosmological parameters. ApJS. 148, 175–194, 2003.

Springel, V., Yoshida, N., White, S.D.M. GADGET: a code for collisionless and gasdynamical cosmological simulations. NewA 6, 79–117, 2001.

Viana, P.T.P., Kay, S.T., Liddle, A.R., Muanwong, O., Thomas, P.A. The power spectrum amplitude from clusters revisited: $\sigma_8$ using simulations with preheating and cooling. MNRAS 346, 319–326, 2003.